diffusion-fundamentals

The Open-Access Journal for the Basic Principles of Diffusion Theory, Experiment and Application

Diffusion Imaging of the Brain: Technical Considerations and Practical Applications

David G. Norris

FC Donders Centre for Cognitive Neuroimaging
Trigon, Kapittelweg 29
6525 EN Nijmegen
The Netherlands
tel ++ 31 (0)24 36 10649
fax ++ 31 (0)24 36 10652
email David.Norris@FCDonders.ru.nl

Abstract

This chapter presents a brief introduction to the application of diffusion-weighted magnetic resonance imaging (MRI) to in vivo studies. Diffusion-weighted MRI has found application both in the clinic, and in basic neuroscience. In the former situation it is primarily used for the detection of brain lesions, in particular infarcted regions. The ability to follow fibre tracts in white matter via diffusion tensor imaging has also made this methodology of interest to the neurosurgeon wishing to avoid severance of essential fibre tracts, but also of interest to the cognitive neuroscientist exploring anatomical connectivity in the brain. The chapter starts with a brief recap of the theory of diffusion-weighted MRI and moves on to examine the two major experimental confounds, eddy currents and bulk motion. Current correction schemes for these problems are touched upon. Diffusion anisotropy is introduced as a potential source of artefacts for lesion detection in white matter, and the diffusion tensor model presented. The chapter concludes with a short introduction to fibre tracking.

1 Introduction

Diffusion weighted NMR experiments performed on living systems including whole body imaging of humans are capable of probing molecular displacements in vivo in the micrometer range. With the exception of NMR microscopy this lies well under the spatial resolution of NMR imaging experiments, in the case of whole-body imaging systems by about three orders of magnitude. Diffusion weighted imaging (DWI) thus offers a unique opportunity for obtaining information from morphologies otherwise inaccessible to the NMR imaging method. Diffusion weighted imaging has been shown to have significant clinical relevance in both the early detection of infarcts [1], (an example of which is given in Figure 1) and in other pathologies. The acquisition of the full diffusion tensor information makes possible in vivo fibre tracking in the white matter of the brain.

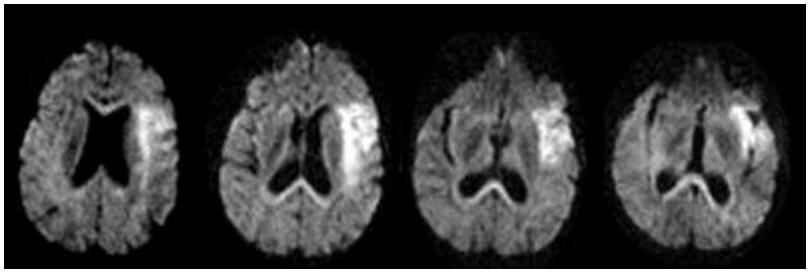

Figure 1. Diffusion-weighted echo planar images obtained three hours post infarction clearly show the infarcted region as a hyper-intense area.

2 Theory

If the effects of relaxation are neglected then the equation of motion for the transverse magnetization $\mathbf{M}_{XY}(\mathbf{r},t)$ in the presence of a constant magnetic field gradient is given by the modified Torrey-Bloch equation (2):

$$\frac{\partial \mathbf{M}_{xy}(\mathbf{r},t)}{\partial t} = i\gamma \mathbf{G}.\mathbf{r}\mathbf{M}_{xy}(\mathbf{r},t) + D\nabla^2 \mathbf{M}_{xy}(\mathbf{r},t)\,. \qquad (1)$$

The solution of this equation gives the well known result that

$$\mathbf{M}_{xy}(\mathbf{r},t) = M_0 \exp(-i\gamma \mathbf{G}.\mathbf{r}t)\exp(-\gamma^2 |\mathbf{G}|^2 Dt^3/3)\,, \qquad (2)$$

i.e. the attenuation coefficient of the NMR signal is proportional to the square of the gradient strength, and to the cube of the gradient duration. For a spin echo experiment with $t = 2\tau$, and in which the gradient is constantly present then the phase term disappears to give

$$\mathbf{M}_{xy}(\mathbf{r},t) = M_0 \exp(-2\gamma^2 |\mathbf{G}|^2 D\tau^3/3)\,. \qquad (3)$$

Diffusion weighting is usually introduced by means of pulsed magnetic field gradients, essentially so that RF pulses can be applied in the absence of any gradient. The most commonly used experiment is the pulsed gradient spin echo [3] illustrated in Figure 2a, however the alternative stimulated echo experiment (Figure 2b) may be preferred for high diffusion weightings. The latter is only advantageous if the reduction in echo time afforded by the larger value of Δ more than compensates for the 50% signal loss associated with the use of stimulated echoes.

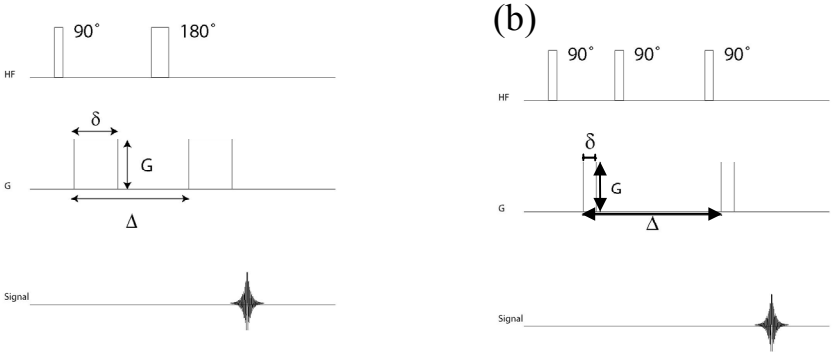

Figure 2 The pulsed gradient spin echo (a) and the pulsed-gradient stimulated echo experiment (b)

The signal attenuation in these experiments is obtained by solving equation (1) for the time varying gradient forms shown in fig. 2, and is given by

$$\mathbf{M}_{xy}(\mathbf{r},t)=M_0\exp\left[-D\left(\gamma|\mathbf{G}_0|\delta\right)^2\left(\Delta-\frac{\delta}{3}\right)\right], \tag{4}$$

where the parameters are as defined in figure 2, and $\Delta-\delta/3$ is the diffusion time (τ). This parameter is of significance because it is related to the square of the expectation value of the molecular displacement by the relation

$$\left\langle \mathbf{r}^2 \right\rangle = 6D\tau, \tag{5}$$

i.e. the gradient timing as programmed into the NMR experiment determines the scale of molecular displacements examined.

Equation (4) is generally called the Stejskal-Tanner equation after its inventors, and in biomedical imaging is often written in the form

$$\mathbf{M}_{xy}(\mathbf{r},t)=M_0\exp(-bD), \tag{6}$$

where the *b*-value for a particular nucleus is determined by the gradient strength and timing.

3 Experimental problems

3.1 Eddy currents

There are a number of experimental confounds that are of particular importance for diffusion-weighted imaging, the first of these are eddy currents. Diffusion measurements are vulnerable to eddy current effects because of the large gradient pulses used. It is only the eddy currents with long time constants that need to be taken into account, but these

can significantly affect diffusion experiments. This means that even systems with good-quality self-shielded gradients suffer from eddy currents. The low bandwidth along the phase-encoding direction makes the commonly used echo planar imaging sequence [4] particularly vulnerable to eddy currents. The strategies for compensating eddy currents rely either on the acquisition of additional data in order to obtain correction parameters for post-processing, or to modify the diffusion weighting experiment to produce fewer eddy currents, for example by using double bipolar gradient pulses as illustrated in Figure 3. The physical basis for this scheme is that the adjacent bipolar gradient pulses produce opposite eddy currents in the cryostat, but have a cumulative effect with respect to diffusion weighting [5]. The total sensitivity of the scheme for diffusion weighting is barely reduced, and given by

$$b = (2\delta\gamma G)^2\left(\Delta - \frac{a}{2} - \frac{2\delta}{3}\right). \qquad (7)$$

For imaging performed at a given echo time it is further possible to optimise the precise timing of the scheme so that the eddy currents occurring during the imaging experiment are minimised [6].

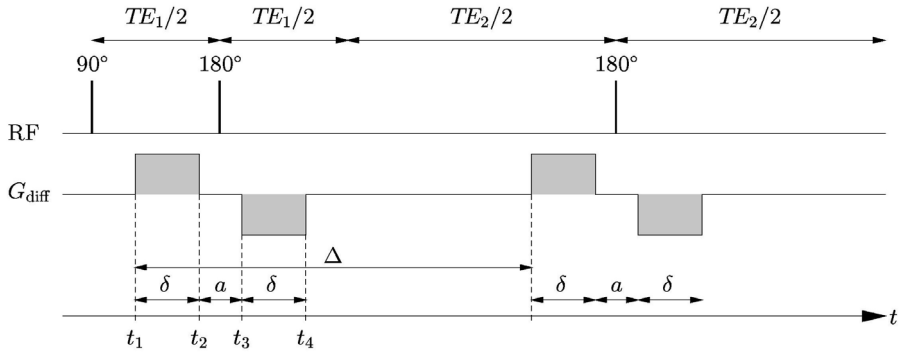

Figure 3. Bipolar diffusion weighting scheme for the minimisation of eddy currents.

3.2 Bulk motion

Given that the diffusion weighting sensitises the imaging experiment to motion on the micrometer level it is hardly surprising that bulk motion presents a serious confound to diffusion weighted imaging. For displacement of the object it is well known that the pulsed gradient spin echo (PGSE) sequence as shown in Figure 2a will give rise to a velocity dependent phase change of

$$\Phi = \gamma\delta\Delta\mathbf{G}.\mathbf{v} \qquad (8)$$

To produce a significant diffusion attenuation it is generally considered necessary to achieve *b*-values in the range 500-1000 s mm^{-2}, for example parameters of G=40 mT/m; δ=20 ms and Δ=30 ms will give a *b*-value of 598 s mm^{-2} for protons. These parameters will result in a phase change of π for a velocity of only 0.5 mm/s. The motion of a rigid body may be described completely in terms of translation and rotation.

The effect of rotation was first examined by Anderson and Gore for small rotations [7]. The general effect of rotation is to produce a phase gradient in the object by the mechanism sketched in Figure 4. The phase gradient in the object is best viewed in the plane perpendicular to the axis of rotation, and is perpendicular both to the axis of rotation and to the component of the diffusion weighting gradient within the plane. The vector $\mathbf{r}_\varphi$ denoting the phase gradient is then given by

$$\mathbf{r}_\phi = \gamma \mathbf{G} \times \mathbf{\Omega}\,, \qquad (9)$$

where **G** and **Ω** denote the directions of the diffusion weighting gradient and of the rotation vector, respectively. In diffusion weighting sequences where the direction of **G** is a function of time, the phase gradient over the object at the end of the diffusion weighting period may be obtained by suitably modifying equation (9).

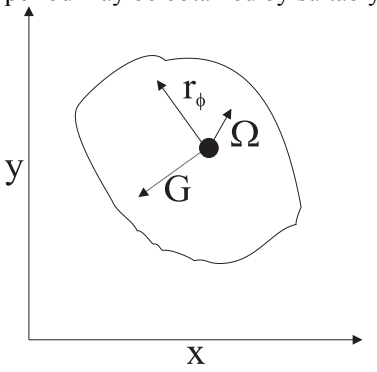

Figure 4. The rotation vector **Ω** for an object rotating about an axis of arbitrary orientation relative to the gradient direction, is shown, as is the relationship between this vector, the orientation of the diffusion weighting gradient **G** and the resultant phase gradient across the object $\mathbf{r}_\varphi$.

The simplest method of avoiding motion artifacts is to use a motion-insensitive method such as EPI (echo planar imaging). Non single-shot experiments are affected by the phase differences between acquisitions, and hence require some correction in order to obtain an artifact-free image. The most promising approach for doing this is the navigator echo correction method [8]. The basis of navigator correction is to acquire an additional non phase-encoded echo, which is then used to correct the phase of all other echoes acquired as a result of a single excitation. The effects of both displacement and rotation can only be adequately corrected with a single navigator if the diffusion sensitising gradient and the phase-encoding gradient are parallel [7]. In this situation rotation produces a phase gradient in the final image parallel to the read direction and hence no signal loss, whereas if this phase gradient is perpendicular to the readout direction then it will result in dephasing. If complete freedom in the direction of the diffusion sensitising gradient is

required then a second navigator echo can be applied, perpendicular to the first: this gives information about the strength of the phase gradient, which is equivalent to a shift of the data in k-space [9]. The data may then be regridded to produce a final image. Despite the clear improvements introduced by navigator echoes, ECG and respiratory gating are still necessary, because the motion of the brain can be that of a non-rigid body in the first few hundred milliseconds after the R-wave of the ECG [10].

4 Anisotropy and diffusion tensor imaging

A systematic ordering of cells, which is significant on the scale of an imaging voxel will cause the diffusion to be anisotropic. This occurs in the white matter of the brain: here the diffusion coefficient is no longer a scalar quantity, but a tensor [11]. The reason for this is the limited permeability of the cell membrane, that causes the expectation value for the displacement to be greater along the direction of the axon as illustrated in Figure 5a. The effect of this on diffusion-weighted images is shown in figures 5b and 5c.

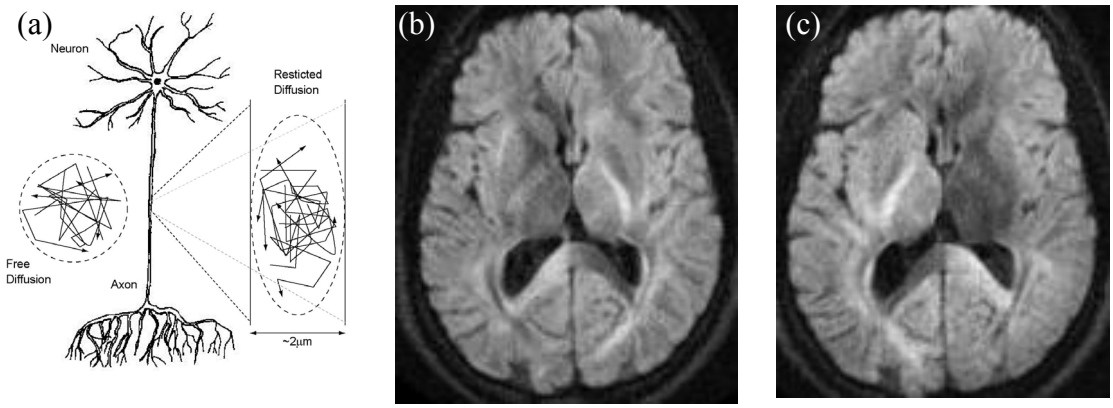

Figure 5. The origin and effect of anisotropy in white matter. (a) sketches of an axon and the effect on the expectation value of the displacement. (b) and (c) show diffusion-weighted images with the weighting along (x,y) and (x,-y), respectively.
The expression describing the signal attenuation is given by:

$$\log\left(\frac{S(b)}{S(0)}\right) = -\sum_{i=x,y,z}\sum_{j=x,y,z} b_{ij} D_{ij} \,, \tag{10}$$

where:

$$b_{ij} = \int_0^\tau k_i(t) k_j(t) dt; \; k_i(t) = \int_0^t \gamma G_i(t') dt' \,, \tag{11}$$

and the D_{ij} represent the elements of a symmetrical tensor. It is now conventionally assumed that the eigenvector with the largest corresponding eigenvalue is the principal diffusive direction of the axon.

Because of the symmetry of the tensor only 6 coefficients have to be measured to determine the complete diffusion tensor. This is being done by the application of 6 different diffusion gradients. A typical set of gradient vectors could be: (1 0 1); (-1 0 1); (0 1 1); (0 1 –1); (1 1 0) and (-1 1 0), all normalized with respect to amplitude G.

Equation 10 can now, for the first gradient direction, be expressed as:

$$A = b_{xx}D_{xx} + b_{yy}D_{yy} + b_{zz}D_{zz} + 2(b_{xy}D_{xy} + b_{xz}D_{xz} + b_{yz}D_{yz}) \tag{12}$$

with A = -log(S(b)/S(0)).

After the 6 measurements a set of 6 linear equations with 6 unknown variables is obtained which can be formulated as follows:

$$\begin{pmatrix} A^{(1)} \\ A^{(2)} \\ A^{(3)} \\ A^{(4)} \\ A^{(5)} \\ A^{(6)} \end{pmatrix} = \begin{pmatrix} b_{xx}^{(1)} & b_{yy}^{(1)} & b_{zz}^{(1)} & 2b_{xy}^{(1)} & 2b_{xz}^{(1)} & 2b_{yz}^{(1)} \\ b_{xx}^{(2)} & b_{yy}^{(2)} & b_{zz}^{(2)} & 2b_{xy}^{(2)} & 2b_{xz}^{(2)} & 2b_{yz}^{(2)} \\ b_{xx}^{(3)} & b_{yy}^{(3)} & b_{zz}^{(3)} & 2b_{xy}^{(3)} & 2b_{xz}^{(3)} & 2b_{yz}^{(3)} \\ b_{xx}^{(4)} & b_{yy}^{(4)} & b_{zz}^{(4)} & 2b_{xy}^{(4)} & 2b_{xz}^{(4)} & 2b_{yz}^{(4)} \\ b_{xx}^{(5)} & b_{yy}^{(5)} & b_{zz}^{(5)} & 2b_{xy}^{(5)} & 2b_{xz}^{(5)} & 2b_{yz}^{(5)} \\ b_{xx}^{(6)} & b_{yy}^{(6)} & b_{zz}^{(6)} & 2b_{xy}^{(6)} & 2b_{xz}^{(6)} & 2b_{yz}^{(6)} \end{pmatrix} \cdot \begin{pmatrix} D_{xx} \\ D_{yy} \\ D_{zz} \\ D_{xy} \\ D_{xz} \\ D_{yz} \end{pmatrix} \tag{13}$$

The elements of the diffusion tensor can be obtained from this set of equations by means of a simple linear regression.

Anisotropy can also confound the detection of lesions, and its effects can best be eliminated if the trace of the diffusion tensor is obtained, either by taking the sum of three perpendicular measurements, or by using a single shot trace measurement. A commonly used scalar representation of the degree of anisotropy is the fractional anisotropy [12] given by

$$FA = \frac{\sqrt{3\left[\left(\lambda_1 - \langle\lambda\rangle\right)^2 + \left(\lambda_2 - \langle\lambda\rangle\right)^2 + \left(\lambda_3 - \langle\lambda\rangle\right)^2\right]}}{\sqrt{2\left(\lambda_1^2 + \lambda_2^2 + \lambda_3^2\right)}} \tag{14}$$

Where the λ_i are the eigenvalues and

$$\langle\lambda\rangle = \left(\lambda_1 + \lambda_2 + \lambda_3\right)/3 \tag{15}$$

Both a trace and a fractional anisotropy image are illustrated in Figure 6.

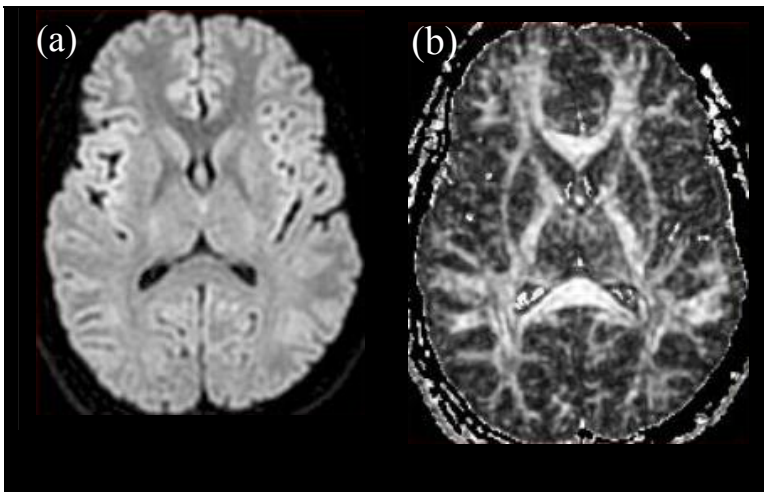

Figure 6. Scalar images obtained from the diffusion tensor (a) trace and (b) fractional anisotropy

5 Biophysics of water diffusion in tissue

The biophysics of water diffusion in tissue is complex. If the vascular network is neglected then both the intra- and extracellular compartments still need to be taken into consideration. The diffusion is hindered by the cell membrane which, although permeable to water, still reflects a significant obstruction to diffusion. In the extracellular system the tortuosity of the diffusion pathways around cells has to be considered. In the intracellular case the diffusion is hindered. In both compartments possible significant non-Brownian contributions to molecular displacements cannot be eliminated. All of these factors can of course be included in mathematical models of diffusion, but it is still difficult to measure the essential parameters that are necessary for such a model to be of value in quantification. The change in the diffusion-weighted signal that occurs upon infarction is primarily believed to arise from an influx of water into the cells that occurs within minutes of occlusion, combined with an increase in extracellular tortuosity. However, simulations have so far failed to accurately predict the change in diffusion coefficient that is measured, and consistently require an additional drop in the intracellular diffusion coefficient. These issues and the associated experiments have been reviewed [13].

6 Incorporation of diffusion weighting in imaging experiments

Successful diffusion-weighted imaging (DWI) imposes a number of requirements on the imaging sequence with which it is to be combined:

(i) The image contrast should ideally be determined by the diffusion and no other contrast parameter.

(ii) The presence of motion causes unpredictable changes in signal phase between repeated applications of the same diffusion-weighting experiment. If the imaging method used relies on multiple excitations then the effects of

motion must either be reduced or corrected. Single-shot imaging experiments have here a clear advantage as they have no reliance on phase-consistency between excitations.

(iii) High-contrast DWI requires a significant signal attenuation from the more rapidly diffusing spins, and attenuates all signal to some extent. A high intrinsic signal to noise ratio (SNR) is hence required from the imaging experiment.

The sequence most frequently used for DWI is single shot EPI. It has attained a pre-eminent position in this field, due to its speed, insensitivity to motion and high sensitivity. The disadvantages of single-shot EPI are a limited spatial resolution and the distortions caused by susceptibility gradients. Alternative sequences to single-shot EPI generally find a niche application, to date none has seemed likely to replace it as the workhorse of DWI. The most commonly used sequence in standard clinical imaging is Fast Spin Echo (FSE), which acquires a string of RF-refocussed independently phase-encoded spin echoes. However, successful implementation of this sequence requires that the CPMG condition be adhered to. The presence of arbitrary phase shifts caused by motion in the diffusion weighting gradients makes this impossible for diffusion-weighted FSE. Schemes for making this sequence independent of the CPMG-condition, and hence motion insensitive, have previously resulted in a 50% loss in sensitivity [14-16]. The development of on-line motion correction techniques [17] using navigators means that this loss is no longer mandatory. However, acquisition during the non-rigid body part of the cardiac cycle must be avoided. As the echo-train-length (ETL) in these sequences is longer than in EPI, data cannot be acquired so fast, and the large number of refocusing pulses required can cause problems of power deposition. However, the sequences are highly sensitive and invulnerable to susceptibility artifacts. A third alternative is the FLASH (fast low angle shot) imaging sequence, based on a string of short TR, low excitation angle, gradient echoes. Here, the diffusion-weighting preparation experiment is required to produce longitudinal magnetisation. This may be achieved by means of a DEFT (driven equilibrium fourier transform) preparation experiment, which in its unmodified form is vulnerable to motion [18], or by using STEAM (stimulated echo acquisition mode), which intrinsically offer only 50% of the possible sensitivity [19]. The DEFT experiment can be made motion-insensitive in a similar fashion to FSE [20], or alternatively on-line motion correction can be applied [21]. Although the FLASH experiment is less sensitive than EPI it is far less vulnerable to susceptibility artefacts. Furthermore, as the prepared magnetisation decays with T_1 a larger data matrix may be acquired after a single diffusion weighting experiment than would be possible with EPI or FSE.

Segmented acquisition schemes may be used with all the sequences outlined above. They generally offer an improved spatial resolution at the cost of lengthened experimental durations and the requirement to correct for motion between segments. For EPI, any reduction in ETL will also reduce image distortion.

In the recent past, radial k-space schemes have attracted considerable attention. The attraction of the classical projection reconstruction method is that no phase encoding is performed, and the method is insensitive to phase errors caused by motion. However, rotational motion may still cause signal loss if a component of the diffusion-weighting

gradient is parallel to the readout direction. Radial k-space acquisition also has the advantage that the centre of k-space is sampled repeatedly; giving an averaging effect that reduces the sensitivity to motion, and gives the possibility of inherent navigator correction.

7 Fibre tracking

A popular use for diffusion tensor imaging is the production of tractograms depicting the course of fibre tracts in white matter. Numerous algorithms have been published, and these can essentially be divided into two categories: Those that attempt to track the fibres directly, hence are capable of producing estimates of where the tracts are positioned, [22] and those that use the anisotropic data to produce probabilistic estimates as to whether two regions of grey matter are connected with each other [23,24]. Examples of each method are shown in Figure 7.

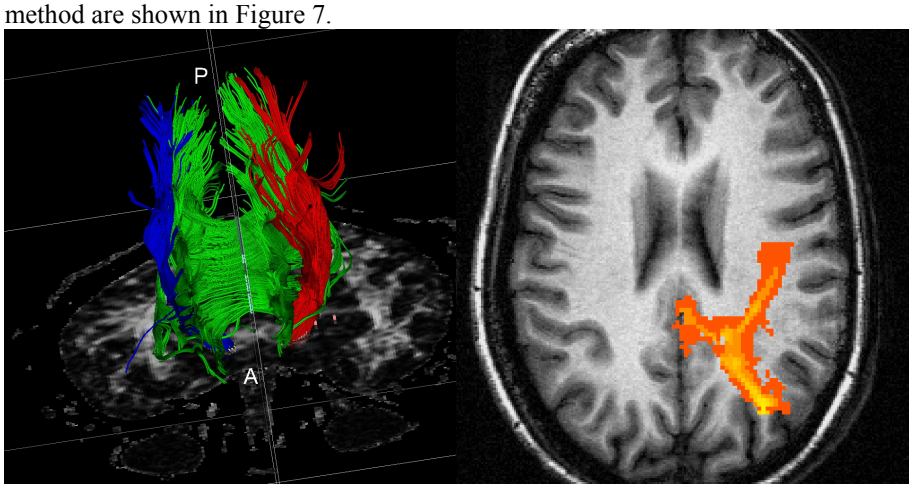

Figure 7. Left is the result of a line-streaming algorithm, right a probabilistic result. In both images the paths through the white matter are represented in colour. In the left image the different colours represent different seed regions.

8 Conclusions

Diffusion imaging of the brain has proven to be of major significance in both clinical and neuro-cognitive fields of application, there are still many technical issues that will require attention in coming years. One of these is the issue of validation with respect to fibre tracking: the uniqueness of the method is in many ways almost a disadvantage in this respect, as there is no real gold-standard, particularly for the human brain, with which results can be compared. The issue of bulk motion is significant, especially in many soft tissues of the body where the motion is any-thing but rigid-body in nature. The limited resolution of single-shot imaging experiments may be overcome in the near future by the introduction of parallel imaging techniques, in which some of the spatial encoding is performed by exploiting the differing spatial sensitivity profiles of multiple RF receiver coils. There are now a number of techniques which attempt to resolve multiple fibre

directions within a single voxel, and it is to be expected that these methods will be combined with more complete fibre-tracking methods within the coming years. Some attempts have recently been made to follow the white matter tracts into the cortex, and further energy may well be expended on this activity in the future.

In conclusion, diffusion-weighted magnetic resonance imaging represents a beautiful synthesis of magnetic resonance methodology, diffusion biophysics and clinical and neuro-scientific application. It already provides great service in many realms of application and this can only be expected to expand in significance in the future.

Acknowledgements

The author would like to thank Martin A Koch and Hubert Fonteijn for contributing material used in this text.

References

(1) ME Moseley, Y Cohen, J Mintorovitch, L Chileuitt, H Shimizu, J Kucharczyk, MF Wendland, PR Weinstein: Early detection of regional cerebral ischemia in cats: comparison of diffusion- and t2-weighted MRI and spectroscopy. Magn. Reson. Med. 14 (1990) 330-46.

(2) HC Torrey: Bloch Equations with Diffusion Terms. Phys. Rev. 104 (3) (1956) 563-65.

(3) EO Stejskal, JE Tanner: Spin diffusion measurements: spin echoes in the presence of a time-dependent field gradient. J. Chem. Phys. 42 (1965) 288-92.

(4) P Mansfield: Multi-planar image formation using NMR spin echoes. J Phys C: 10 (1977) L55-L58.

(5) G Wider, V Dötsch, K Wüthrich: Self-compensating pulsed magnetic-field gradients for short recovery times. J Magn Reson A 108 (1994) 255-58.

(6) TG Reese, O Heid, RM Weisskoff, VJ Wedeen: Reduction of eddy-current-induced distortion in diffusion MRI using a twice-refocused spin echo. Magnetic Resonance in Medicine 49 (2003) 177-82.

(7) AW Anderson, JC Gore: Analysis and correction of motion artifacts in diffusion weighted imaging. Magn. Reson. Med. 32 (1994) 379-87.

(8) RJ Ordidge, JA Helpern, ZX Qing, RA Knight, V Nagesh: Correction of motional artifacts in diffusion-weighted MR images using navigator echoes. Magn. Reson. Imaging 12 (1994) 455-60.

(9) K Butts, A de Crespigney, JM Pauly, M Moseley: Diffusion-weighting interleaved echo-planar imaging with a pair of orthogonal navigator echoes. Magn. Reson. Med. 35 (1996) 763-70.

(10) D Greitz, R Wirestam, A Franck, B Nordell, C Thomsen, F Stahlberg: Pulsatile brain movement and associated hydrodynamics studied by magnetic resonance phase imaging. the Monro-Kellie doctrine revisited. Neuroradiology 34 (1992) 370-80.

(11) PJ Basser, J Mattiello, D Le Bihan: Estimation of the effective self-diffusion tensor from the NMR spin-echo. J. Magn. Reson. 103B (1994) 247-54.

(12) PJ Basser, C Pierpaoli: Microstructural and physiological features of tissues elucidated by quantitative-diffusion-tensor MRI. Journal of Magnetic Resonance Series B 111 (1996) 209-19.
(13) DG Norris: The effects of microscopic tissue parameters on the diffusion weighted magnetic resonance imaging experiment. NMR Biomed 14 (2001) 77-93.
(14) DG Norris, P Börnert, T Reese, D Leibfritz: On the application of ultra-fast RARE experiments. Magn Reson Med 27 (1992) 142-64.
(15) F Schick: SPLICE: sub-second diffusion-sensitive MR imaging using a modified fast spin-echo acquisition mode. Magn Reson Med 38 (1997) 638-44.
(16) DC Alsop: Phase insensitive preparation of single-shot RARE: application to diffusion imaging in humans. Magn. Reson. Med. 38 (1997) 527-33.
(17) DG Norris, W Driesel: Online motion correction for diffusion-weighted imaging using navigator echoes: application to RARE imaging without sensitivity loss. Magn Reson Med 45 (2001) 729-33.
(18) WH Perman, M Gado, JC Sandstrom, DPSF: snapshot FLASH diffusion/perfusion imaging, Proceedings: 9th annual meeting of the society of magnetic resononance in medicine, New York, 1990, p. 309.
(19) KD Merboldt, W Hänicke, H Bruhn, ML Gyngell, J Frahm: Diffusion imaging of the human brain in vivo using high-speed STEAM MRI. Magn Reson Med 23 (1992) 179-92.
(20) U Sinha, S Sinha: High speed diffusion imaging in the presence of eddy currents. J Magn Reson Imag 6 (1996) 657-66.
(21) KS Weih, W Driesel, M von Mengershausen, DG Norris: Online motion correction for diffusion-weighted segmented-EPI and FLASH imaging. Magma 16 (2004) 277-83.
(22) S Mori, BJ Crain, VP Chacko, PCM van Zijl: Three-dimensional tracking of axonal projections in the brain by magnetic resonance imaging. Annals of Neurology 45 (1999) 265-69.
(23) MA Koch, DG Norris, M Hund-Georgiadis: An investigation of functional and anatomical connectivity using magnetic resonance imaging. Neuroimage 16 (2002) 241-50.
(24) TEJ Behrens, H Johansen-Berg, MW Woolrich, SM Smith, CAM Wheeler-Kingshott, PA Boulby, GJ Barker, EL Sillery, K Sheehan, O Ciccarelli, AJ Thompson, JM Brady, PM Matthews: Non-invasive mapping of connections between human thalamus and cortex using diffusion imaging. Nature Neuroscience 6 (2003) 750-57.